NASA-CR-200853

Analysis of residual acceleration effects on transport and segregation during directional solidification of tin-bismuth in the MEPHISTO furnace facility

Annual Progress Report
for NASA grant NAG3 1740
March 1995-March 1996

Prepared by J. Iwan D. Alexander, Principal Investigator
Center for Microgravity and Materials Research
University of Alabama in Hunstville
Huntsville, Alabama 35899

1. Introduction

The object of this work, started in March of 1995, is to approach the problem of determining the transport conditions (and effects of residual acceleration) during the plane-front directional solidification of a tin-bismuth alloy under low gravity conditions. The work involves using a combination of 2- and 3-D numerical models, scaling analyses, 1D models and the results of ground-based and low-gravity experiments. The latter are to be conducted during the MEPHISTO experiment scheduled for USMP-3 in early 1996. The models will be used to predict the response of the transport conditions and consequent solute segregation in directionally solidifying tin-bismuth melt. Real-time Seebeck voltage variations across a Sn-Bi melt during directional solidification in MEPHISTO on USMP-1 show a distinct variation which can be correlated with thruster firings. The Seebeck voltage measurement is related to the response of the instantaneous average melt composition at the melt-solid interface. This allows a direct comparison of numerical simulations with the Seebeck signals obtained on USMP-1. The effects of such accelerations on composition for a directionally solidifying Sn-Bi alloy have been simulated numerically. USMP-1 acceleration data was used to assist in our choice of acceleration magnitude and orientation. The results show good agreement with experimental observations. The USMP-3 experiments took place earlier this year (February 22 through March 6). There were several differences between the USMP-3 experiments as compared to USMP-1. Firstly a more concentrated alloy was solidified and, secondly, Primary Reaction Control System thruster burns were requested at particular times during four separate growth runs. This allowed us to monitor the response Seebeck response under well-characterized growth conditions. In addition, we carried out simulations during the experiment in order to interpret the Seebeck signal. Preliminary results are described below.

2. First year accomplishments

A sketch of the experiment set-up is shown in Fig. 1. There are two furnaces, one is fixed the other is translated through a temperature gradient. The applied temperature profile shown in Fig. 1 leads to a central cylindrical melt volume bounded by a moving and a stationary (or reference) solid-liquid interface. The melt composition at the moving and the stationary reference interfaces is not the same. For Sn-Bi there is a dependence of melting temperature on concentration. Thus, it follows that the melting temperature at the two interfaces will not be the same. The Seebeck effect gives rise to a small but measurable voltage difference between these two interfaces. Measurement of this voltage difference allows the determination of the average temperature and, thus, the average composition of at the growing interface. The MEPHISTO set-up and the Seebeck measurements are discussed in more detail in [11].

The basic model system used for the simulations has been described elsewhere [1,2]. The essential features are outlined below. Solidification takes place as the ampoule is translated along a temperature gradient. For this model system, translation of the ampoule is simulated by supplying a doped melt of bulk composition c_∞ at a constant velocity V_g at the top of the computational space (inlet), and withdrawing a solid of composition $c_s = c_s(\boldsymbol{x},t)$ from the bottom. The crystal-melt interface is located at a distance L from the inlet; the width of the ampoule is W. The temperature at the interface is taken to be T_m, the melting temperature of the crystal, while the upper boundary is held at a higher temperature T_h. The ampoule wall temperatures are prescribed according to the particular situation to be modelled. Since we wish to confine our attention to compositional nonuniformities caused by buoyancy-driven convection, rather than variations resulting from non-planar crystal-melt interfaces, the interface is held flat. We expect that, given the large (175 -195 K cm^{-1}, temperature gradient) that changes in melting temperature due to compositional non-uniformity will not lead to significant changes in interface shape due to interfacial compositional inhomogeneity. In addition, because of the melt's low Prandtl number together with the low magnitude accelerations, convection does not lead to significant deviations of the temperature from the conductive state and, thus, changes in the interface shape due to changes in the thermal field will be negligible. The governing equations governing coupled convective-diffusive heat mass and species transfer in the melt are taken to be the Oberbeck-Boussinesq equations which are solved using a Chebeyshev spectral method.

In an actual experiment, owing to the finite length of the ampoule, there is a gradual decrease in length of the melt zone during growth. In this model, transient effects related to the change in melt length are ignored. This assumption is referred to as the quasi-steady assumption and is frequently used in melt-growth modelling. Since the MEPHISTO experiments involves melt lengths that are far in excess of the ampoule diameter, this does not preclude us form calculating the compositional transient. That is we can start the calculations by solidifying from an initially uniform composition melt. Our results, when compared to experiment, reveal that this assumption is justified. The thruster firings are simulated using impulsive accelerations which are introduced through the time-dependent body-force term $\boldsymbol{g}$.

During the first year of this grant we calculated the response of the system to impulsive accelerations of various magnitudes and durations our preliminary results are described in [4] (see attached publication in the appendix).

During the recent USMP-3 experiments the first quantitative experimental results concerning the effects of microgravity disturbances on the directional solidification. An example of the simulations made during the USMP-3 experiment and comparison with the real-time (raw, uncorrected) Seebeck signal is shown in Fig. 1. Our results are the subject of a publication which will be submitted to the Journal of crystal growth in the near future.

References

[1] J.I.D. Alexander, J. Ouazzani and F. Rosenberger, J. Crys. Growth 97 (1989) 285.

[2] J.I.D. Alexander, S. Amiroudine, J. Ouazzani and F. Rosenberger, J. Crys. Growth 113 (1991) 21.

[3] J.-J. Favier and A. Rouzaud, Revue Phys. Appl. 22 (1987) 713.

[4] J.I.D. Alexander, *Response of Crystal Growth Experiments to Time-Dependent Residual Acceleration*, Proceedings of the 9th European Symposium on Gravity Dependent Phenomena in Physical Sciences, Lecture Notes in Physics (Springer, Berlin, 1995).

3. Publications

[1] J.I.D. Alexander, Response of Crystal Growth Experiments to Time-Dependent Residual Acceleration, to appear in Proceedings of the 9th European Symposium on Gravity Dependent Phenomena in Physical Sciences, Lecture Notes in Physics (Springer, Berlin, 1995).

[2] J.I.D. Alexander, Scaling and estimation of experiment response to g-jitter, Microgravity Quarterly, Vol. 5, No. 1, 1995.

[3] J.P. Garandet, S. Corre, S. Gavoille, J.J. Favier and J.I.D. Alexander, *On the effect of gravity perturbations on composition profiles during Bridgman crystal growth in space.* to appear, J. Crystal Growth, 1996.

4. Conferences, presentations and papers in preparation

J.I.D. Alexander, "Response of Crystal Growth Experiments to Time-Dependent Residual Acceleration", invited presentation at the Ninth European Symposium on Gravity Dependent Phenomena in Physical Sciences, Berlin, 2-5 May, 1995.

J.I.D. Alexander, Response of solute transport during directional solidification caused by thruster firings: Predictions for the USMP3 MEPHISTO experiment", presented at the Microgravity Measurement Group Meeting, Houston, March 20, 1995.

Computer Simulations of Response to PRCS "Thruster" Burns

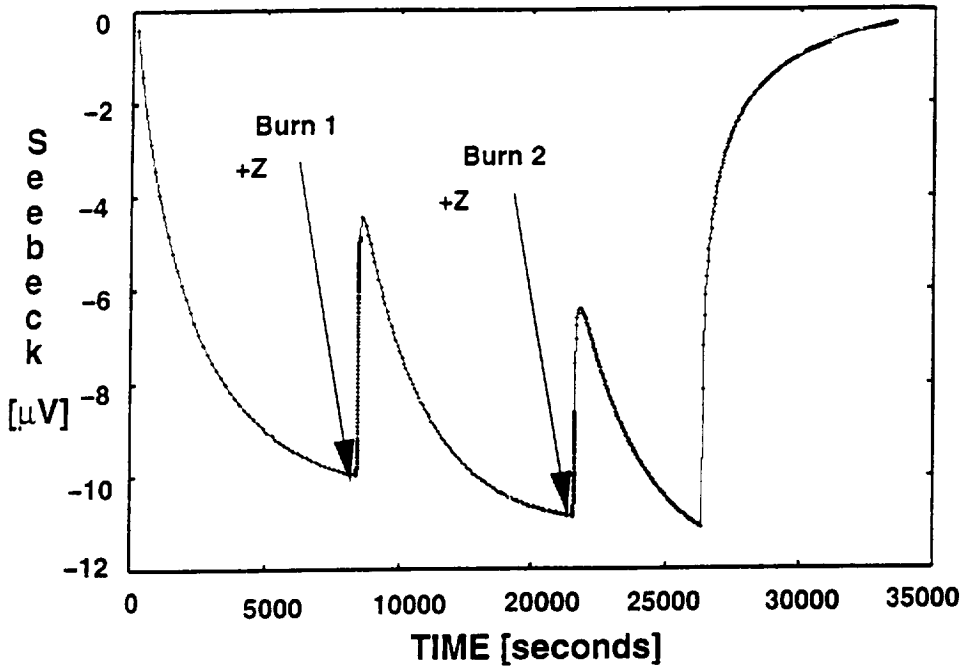

Calculated

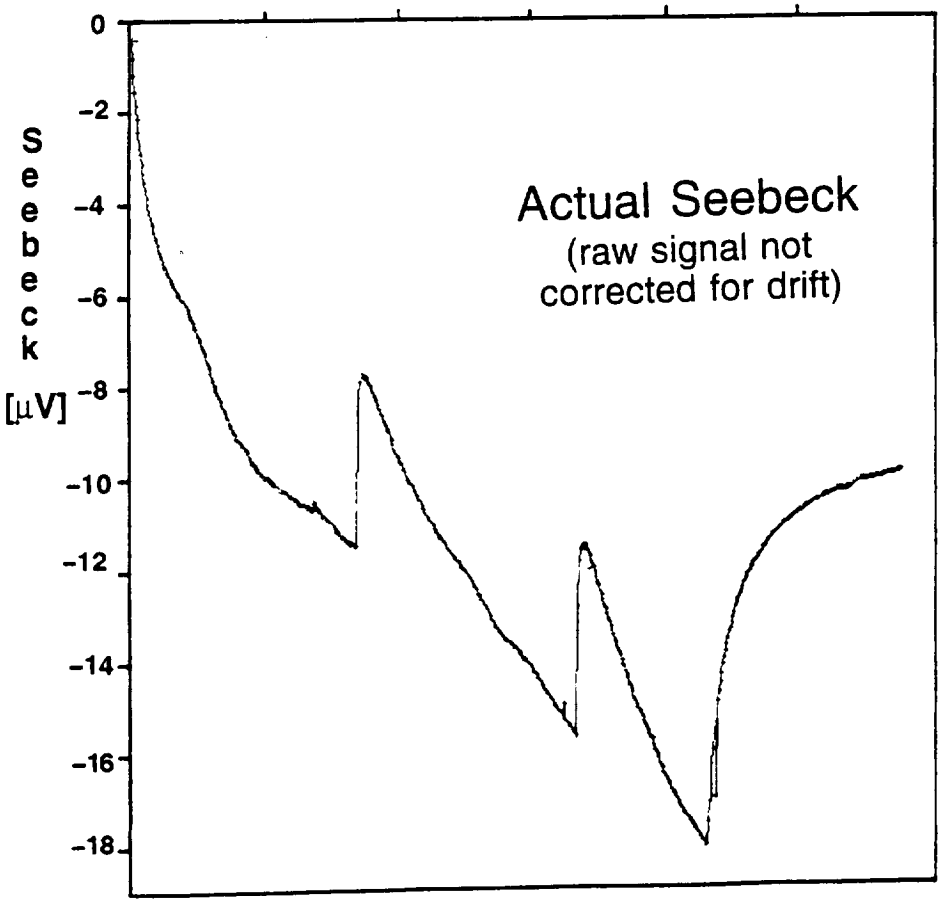

To appear in: *Lecture Notes in Physics*, Vol. 464, Eds. L. Take, H. Walter and B. Feuerbacher, (Springer Verlag, Berlin 1996) pp. 95-104.

Response of Crystal Growth Experiments to Time-Dependent Residual Acceleration

J. Iwan D. Alexander

Center for Microgravity and Materials Research
University of Alabama in Huntsville, Huntsville, Alabama, 35899

Abstract

Real-time Seebeck voltage variations across a Sn-Bi melt during directional solidification in MEPHISTO on USMP-1 show a distinct variation which can be correlated with thruster firings. The Seebeck voltage measurement is related to the response of the instantaneous average melt composition at the melt-solid interface. This allows a direct comparison of numerical simulations with the Seebeck signals obtained on USMP-1. The effects of such accelerations on composition for a directionally solidifying Sn-Bi alloy have been simulated numerically. USMP-1 acceleration data was used to assist in our choice of acceleration magnitude and orientation. Simulation results show reasonable agreement with measured responses although more work is necessary to be able to make a detailed comparison.

Introduction

Under terrestrial conditions, thermally and compositionally inhomogeneous fluids generally give rise to buoyancy-driven flows. In a low-earth-orbit spacecraft, the effective gravity can, in principle, be locally reduced by factors of 10^6 to 10^7 in comparison to conditions at the earth's surface. For crystal growth, this suggests that melt convection, which can lead to undesirable compositional nonuniformity, may be sufficiently reduced to allow diffusive conditions to prevail. Thus, at least for planar melt-crystal growth interfaces, this could lead to lateral or radial composition uniformity in the grown sample. However, it has been recognized for some time [1-3] that residual accelerations arising from the gravity gradient tides, atmospheric drag, vernier firings, crew motions, etc., are sufficient to cause significant deviations from "zero-gravity" conditions. Since the purpose of conducting most low gravity experiments is, generally, to eliminate or substantially reduce convective motion, this has caused some concern. Indeed, it is now apparent from sensitivity studies (for reviews see [4-5] and references therein) that significant composition nonuniformities can arise as a result of residual acceleration or "g-jitter".

The awareness of the potential disruptive effect of g-jitter for crystal growth (and other experiments involving inhomogeneous fluids or fluid surfaces) has spawned a still growing body of literature that deals with the theoretical estimation of g-jitter effects on experiments (see for example [4-9). These estimates range in complexity from order of magnitude analyses to the numerical solution of the full nonlinear equations governing the transport of momentum, heat and mass for systems of interest. The need to measure and record residual acceleration data for use in post-flight assessment of low-gravity experiments has also been recognized. This has led to the development and recent use of several acceleration measurement systems. However, despite the subsequent abundance of acceleration data and the numerous g-jitter analyses, direct experimental correlation of recorded experimental events with g-jitter events is lacking in all but a few cases.

The USMP-1 MEPHISTO experiment involved the directional solidification of a tin-bismuth alloy. During the experiments, acceleration disturbances due to firing of the Orbiter Maneuvering System (OMS) thrusters were recorded which resulted in measurable changes in composition at the growing melt-liquid interface. These changes in composition were measured in real time using Seebeck measurements [10]. In this paper results of simulations of the effect of such thruster firings on transport in Sn-Bi alloys are described. The objective of the work is to better understand the measured response of the interfacial concentration and to plan for future experiments on USMP-3 which will focus on quantifying residual acceleration (g-jitter) effects.

Formulation

A sketch of the experiment set-up is shown in Fig. 1. There are two furnaces, one is fixed the other is translated through a temperature gradient. The applied temperature profile shown in Fig. 1 leads to a central cylindrical melt volume bounded by a moving and a stationary (or reference) solid-liquid interface. The melt composition at the moving and the stationary reference interfaces is not the same. For Sn-Bi there is a dependence of melting temperature on concentration. Thus, it follows that the melting temperature at the two interfaces will not be the same. The Seebeck effect [10,11] gives rise to a small but measurable voltage difference between these two interfaces. Measurement of this voltage difference allows the determination of the average temperature and, thus, the average composition of at the growing interface. The MEPHISTO set-up and the Seebeck measurements are discussed in more detail in [11]. Figure 2. shows the response of the raw Seebeck signal to a 2.7×10^{-2} g acceleration due to an OMS burn during the USMP-1 MEPHISTO experiment.

The basic model system used for the simulations has been described elsewhere [7,8]. The essential features are outlined below. Figure 1 shows the basic model geometry. Solidification takes place as the ampoule is translated along a temperature gradient. For this model system, translation of the ampoule is simulated by supplying a doped melt of bulk composition c_∞ at a constant velocity V_g at the top of the computational space (inlet), and withdrawing a solid of composition $c_S = c_S(\boldsymbol{x},t)$ from the bottom. The crystal-melt interface is located at a distance L from the inlet; the width of the ampoule is W. The temperature at the interface is taken to be T_m, the melting temperature of the crystal, while the upper boundary is held at a higher temperature T_h. The ampoule wall temperatures are prescribed according to the particular situation to be modelled. Since we wish to confine our attention to compositional nonuniformities caused by buoyancy-driven convection, rather than variations resulting from non-planar crystal-melt interfaces, the interface is held flat. The slight change in melting temperature (and, thus, the interface shape) due to composition shifts at the interface following the onset of the convective response to impulsive acceleration are not accounted for in this model.

The governing equations are cast in dimensionless form using L, κ/L (κ is the melt's thermal diffusivity), $\rho_m \kappa^2/L^2$, T_h-T_m, and c_∞ to scale the length, velocity, pressure, temperature, and solute concentration. The dimensionless equations that govern momentum, heat and solute transfer in the melt are then

$$\frac{\partial \mathbf{u}}{\partial t} + (\mathbf{u}\cdot\nabla)\,\mathbf{u} = -\nabla p + Pr\,\nabla^2\mathbf{u} + (Ra\,Pr\,\theta + Ra_s Pr C)\mathbf{g}, \tag{1}$$

$$\nabla\cdot\mathbf{u} = 0, \tag{2}$$

$$\frac{\partial \theta}{\partial t} + \mathbf{u}\cdot\nabla\theta = \nabla^2\theta, \tag{3}$$

$$\frac{Sc}{Pr}\left(\frac{\partial C}{\partial t} + \mathbf{u}\cdot\nabla C\right) = \nabla^2 C, \tag{4}$$

where, $\boldsymbol{u}(\boldsymbol{x},t)$, $\theta = (T(\boldsymbol{x},t) - T_m)/(T_h - T_m)$ and $C = c_m(\boldsymbol{x},t)/c_m^{\infty}$ respectively represent the velocity, temperature and solute concentration. The Prandtl, Rayleigh, Solutal Rayleigh and Schmidt numbers are $Pr = \nu/\kappa$, $Ra = \beta(T_h - T_m)L^3 g/\nu\kappa$, $Ra_S = \beta_c c_m^{\infty} L^3 g/\nu\kappa$ and $Sc = \nu/D$, respectively, and ν is the kinematic viscosity, β and β_c are the thermal and solute expansion coefficients and D is the solute diffusivity. Table 1 gives the values of the physical properties used in these calculations. The term $\boldsymbol{g}$ in (1) specifies the magnitude and orientation of the gravity vector which may be time-dependent. The Rayleigh number is taken to be the value of Ra at the Earth's surface. Thus the magnitude of $\boldsymbol{g}$ is the actual acceleration magnitude relative to 9.8 ms^{-2}.

The following boundary conditions apply at the crystal-melt interface.

$$\begin{aligned} &\theta = 0, \mathbf{u}\cdot\mathbf{N} = \frac{Pe_g Pr}{Sc}, \mathbf{u}\times\mathbf{N} = 0, \\ &\frac{\partial C}{\partial z} = Pe_g(1-k)C, \end{aligned} \tag{5}$$

where $Pe_g = V_g L/D$ and N is the unit vector normal to the planar crystal melt interface. The measure of compositional nonuniformity in the crystal at the interface is defined to be the lateral range in concentration given by

$$\xi(t) = \frac{c_{smax} - c_{smin}}{c_{sav}}\%, \tag{6}$$

where c_s is the (dimensional) solute concentration in the crystal, and c_{av} is the instantaneous average interface concentration. The following boundary conditions are applied at the "inlet"

$$\begin{aligned} &\theta = 1, \mathbf{u}\cdot\mathbf{N} = \frac{Pe_g Pr}{Sc}, \mathbf{u}\times\mathbf{N} = 0, \\ &\frac{\partial C}{\partial x} = Pe_g(C-1) \end{aligned} \tag{7}$$

At the side walls the conditions are (with $\boldsymbol{e}_w$ normal to the walls)

$$\mathbf{u}\,\mathbf{N} = \frac{Pe_g Sc}{Pr}, \quad \mathbf{u}\mathbf{e}_w = 0, \; gradC\cdot\mathbf{e}_w = 0, \tag{8}$$

together with prescribed wall temperature and flux conditions [9,10].

In an actual experiment, owing to the finite length of the ampoule, there is a gradual decrease in length of the melt zone during growth. In this model, transient effects related to the change in melt length are ignored. This assumption is referred to as the quasi-steady assumption and is frequently used in melt-growth modelling. The thruster firings are simulated using impulsive accelerations which are introduced through the time-dependent body-force term $\boldsymbol{g}$. For the OMS burn, the acceleration is suddenly raised up from a nominal level of 10^{-6} g to 2.7×10^{-2} g, and held constant for 35 seconds and then set it back to the nominal level. Other magnitudes and orientations of impulsive accelerations are also examined.

Results

The stream function at different times associated with a 35 second 2.7×10^{-2} g impulse acceleration oriented at 15° to the furnace axis is shown in Fig. 3. The initial condition was diffusion dominated. The 10^{-6} g background acceleration results in negligible flow velocities in comparison to the translation velocity of 2 μm s^{-1}. Under these diffusive conditions, the stream function is steady and is represented by streamlines parallel to the ampoule walls. The concentration profile is laterally uniform and follows the classical exponential profile as it decays into the melt. After the impulse begins, the stream function changes to a single cell pattern as shown in Fig. 3. At 35 seconds (the end of the impulse) the fluid velocities reach a maximum value and then the flow rapidly decays in strength until, at 62 seconds no noticeable deviation from purely diffusive conditions is apparent. The response of the concentration field is shown in Fig. 4 at different times. Note the increase in lateral composition uniformity even after the termination of the disturbance and after the decay of the velocity fields. Furthermore, it is evident that the system has not returned to its initial condition even after 1280 seconds. Indeed, Fig. 5 which depicts the average interface concentration (initial value 3.846) and lateral segregation as a function of time, shows that it will be well in excess of 3000 seconds before the initial conditions are retrieved.

Figure 6 summarizes results for a growth rate of 2 μm s^{-1} for different magnitude and duration impulses oriented parallel to the interface. Here the time has been made dimensionless using $D/k^2\ V_g^2$. This time scale is obtained as follows. The length that must be solidified before the interfacial concentration reaches its steady state value when starting from a melt of constant composition is given by [12] $x^* = D/kV_g$. Taking this to represent approximately the length that must be solidified before steady state is reached following the impulse disturbance we find that the characteristic diffusion time is x^{*2}/D or $D/k^2\ V_g^2$. The curves show that the time taken for the system to completely recover from the impulse acceleration is, at least for the smaller magnitude responses, on the order of $D/k^2\ V_g^2$. For the larger disturbances to the concentration a longer recovery time is necessary. This is probably related to the extent to which the convective flow has carried solute away from the crystal melt interface and into the melt .

Two other features of the curves in Fig. 6 should be mentioned. The first is that, for a given growth velocity, the time taken to reach a minimum value of c_{av} is the same for all cases. The second feature is that for the same value of the product of the acceleration magnitude and duration the history of c_{av} is the same. However, comparison of the actual concentration fields for any given time shows that they are different.

Discussion

Comparison of the simulated response of the average interfacial concentration to the average concentration obtained from the Seebeck measurement shows reasonable agreement. The time taken to reach a minimum average concentration (on the order of 100 seconds in the simulation) and the change in average concentration (38%) agree quite well with the measured response. Evaluation of the predicted time taken for the system to return to its initial state is more difficult due to the fact that when the OMS burn ocurred the system was in a transient. The simualtion predicts that even though the acceleration disturbance lasted only 35 seconds, the concentration disturbance lasted for several thousand seconds. This is consistent with our earlier results [7] for the impact of thruster firing events and is comparable to the characteristic diffusion time for the system. The behavior of the average concentration in response to impulse accelerations is analogous to the response first described by Tiller et al. [12] to a increase in solidification rate from V_1 to V_2 and back to V_1. An important feature of the simulated results which cannot be deduced from the Seebeck measurement is that the lateral interfacial composition nonuniformity, which for a flat interface would normally only arise from convective contributions, continues to increase even after the convective disturbance has died out. This behavior is explained in terms of the influence of diffusion on the coupling between rejection of solute at the (still planar) interface, and the local variation in concentration gradient initially produced by the convective disturbance which sweeps solute out into the melt and decreases the average concentration gradient. The nominal acceleration of 10^{-6} g results in insignificant convective velocities in comparison to the growth velocity and cannot account for this behavior.

Acknowledgments

The author would like to acknowledge support from the National Aeronautics and Space Agency under the grant NAG3 1740 and from the state of Alabama through the Alabama Supercomputing network and the Center for Microgravity and Materials Research. I would also like to thank J.J. Favier and J.P. Garandet for fruitful discussions and for making their experimental data accessible. Thanks are also due to Ahmed Elshabka who undertook some of the calculations.

References

[1] H. Hamacher, R. Jilg and U. Mehrbold, in: Proc. 6th European Symposium on Materials Sciences under Microgravity Conditions, ESA SP-256 (1987) 413.

[2] J. I. D. Alexander and C.A. Lundquist AIAA J. (1988) 193.

[3] M.J.B. Rogers and J.I.D. Alexander and J. Schoess, AIAA J. Spacecraft and Rockets 28 (1992) 52.

[4] R. Monti, J.J. Favier and D. Langbein, in : Fluid Sciences and Materials Sciences in Space, A European Perspective, Ed. H.U. Walter (Springer, Berlin, 1987) 237.

[5] J.I.D. Alexander, Microgravity Science and Technology 3 (1990) 52.

[6] V. I. Polezhaev, A.P. Lebedev, and S.A. Nikitin, Proc. 5th European Symposium on Materials Sciences under Microgravity Conditions, ESA SP-222 (1984) 237.

[7] J.I.D. Alexander, J. Ouazzani and F. Rosenberger, J. Crystal Growth 97 (1989) 285.

[8] J.I.D. Alexander, S. Amiroudine, J. Ouazzani and F. Rosenberger, J. Crystal Growth 113 (1991) 21.

[9] D. Thevenard, and J.J. Favier, Proc. 7th European Symposium on Materials Sciences under Microgravity Conditions, ESA SP-295 (1990) 243.

[10] J.-J. Favier, J.P. Garandet, A. Rouzaud and D. Camel, J. Crystal Growth 140 (1994) 237.

[11] J.-J. Favier and A. Rouzaud, Revue Phys. Appl. 22 (1987) 713.

[12] W. A. Tiller, K.A. Jackson, J.W. Rutter and B. Chalmers, Acta Metall. 1 (1953) 428.

FIGURE CAPTIONS

Fig.1 The MEPHISTO set-up and model system

Fig. 2. Accelerations associated with the OMS firing and the response of the raw Seebeck signal. The sketches indicate the orientation of the acceleration relative to the Orbiter x-axis which is parallel to the axis of the solidifying sample.

Fig. 3 The stream function at different times associated with a 35 second 2.7×10^{-2} g disturbance oriented at 15° to the furnace axis.

Fig. 4 The concentration field at different times associated with a 35 second 2.7×10^{-2} g disturbance oriented at 15° to the furnace axis.

Fig. 5 Average interface concentration (a) and lateral non-uniformity (b) as a function of time associated with a 35 second 2.7×10^{-2} g disturbance oriented at 15° to the furnace axis.

Fig. 6 Average interface concentration as a function of dimensionless time associated with various impulse disturbances.

Table 1 Thermophysical properties

Property	Symbol	Value	
Kinematic Viscosity	ν	2.6×10^{-3}	[$cm^2\ s^{-1}$]
Thermal Diffusvity	κ	0.17	[$cm^2\ s^{-1}$]
Solute Diffusivity	D	1.4×10^{-5}	[$cm^2\ s^{-1}$]
Distribution Coefficient	k	0.26	
Growth Velocity	V_g	2	[$\mu m\ s^{-1}$]

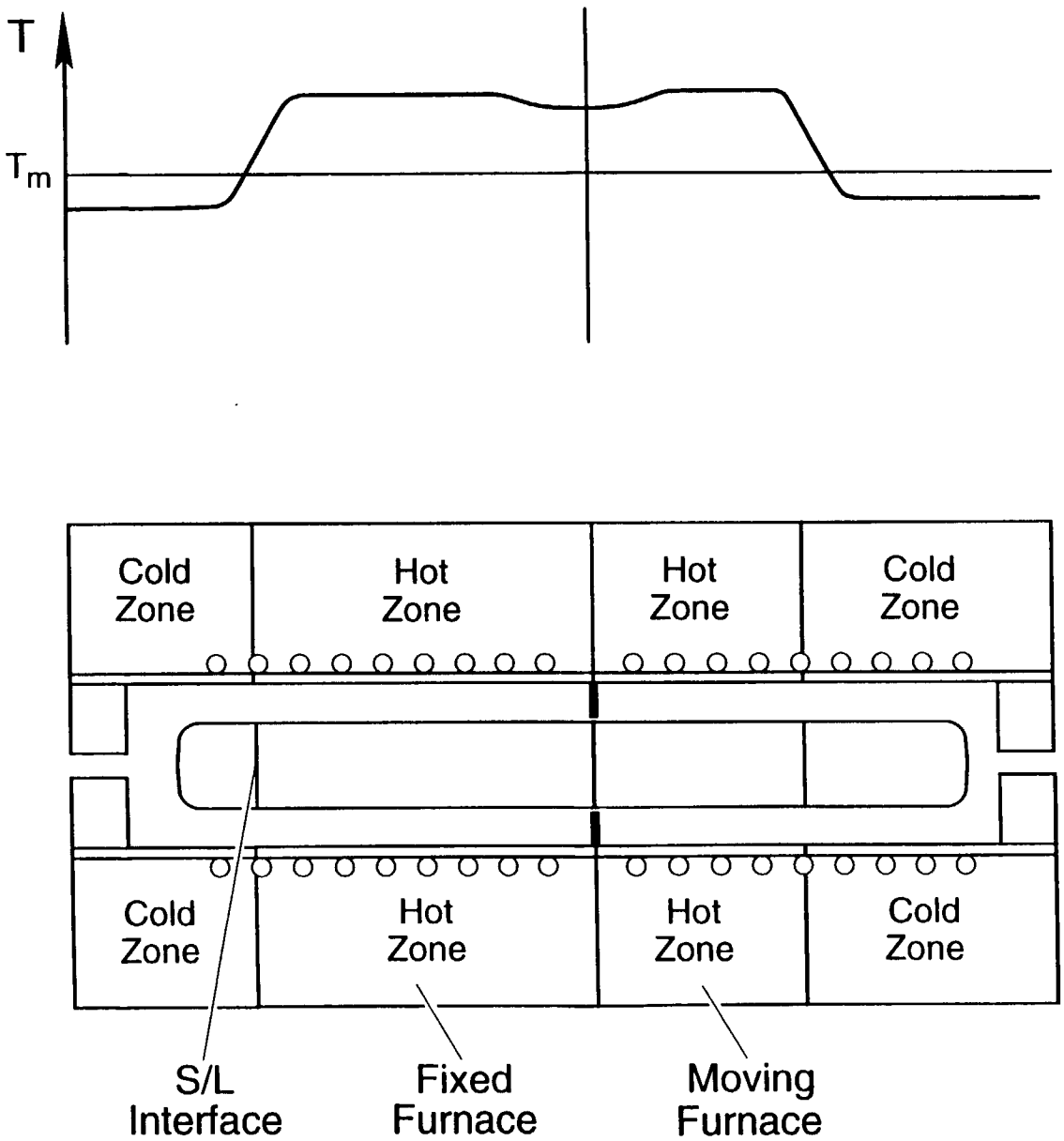
T
T_m
Cold Zone
Hot Zone
Hot Zone
Cold Zone
Cold Zone
Hot Zone
Hot Zone
Cold Zone
S/L Interface
Fixed Furnace
Moving Furnace

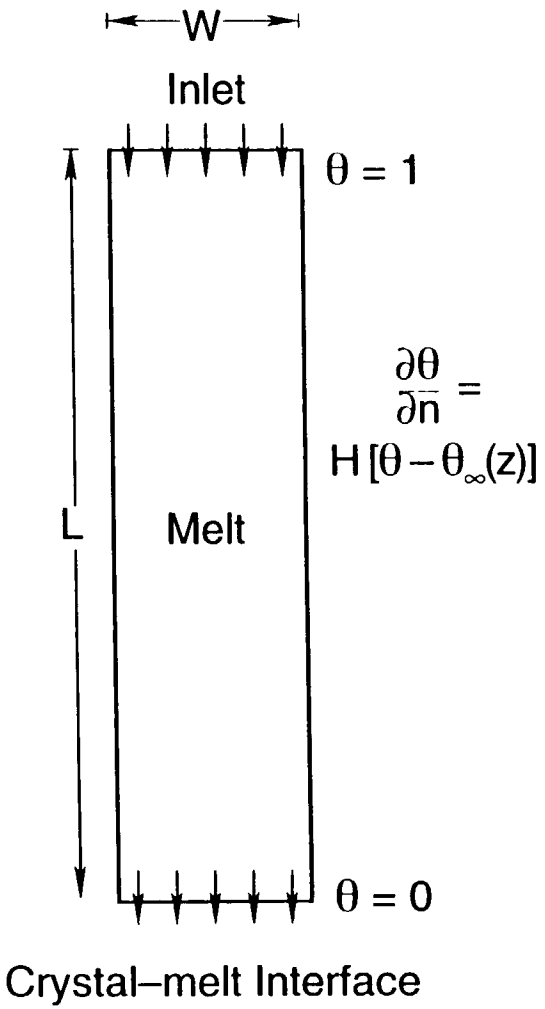
W
Inlet
θ = 1
L
Melt
$\frac{\partial\theta}{\partial\bar{n}} = H[\theta - \theta_\infty(z)]$
θ = 0
Crystal–melt Interface

FIG. 1

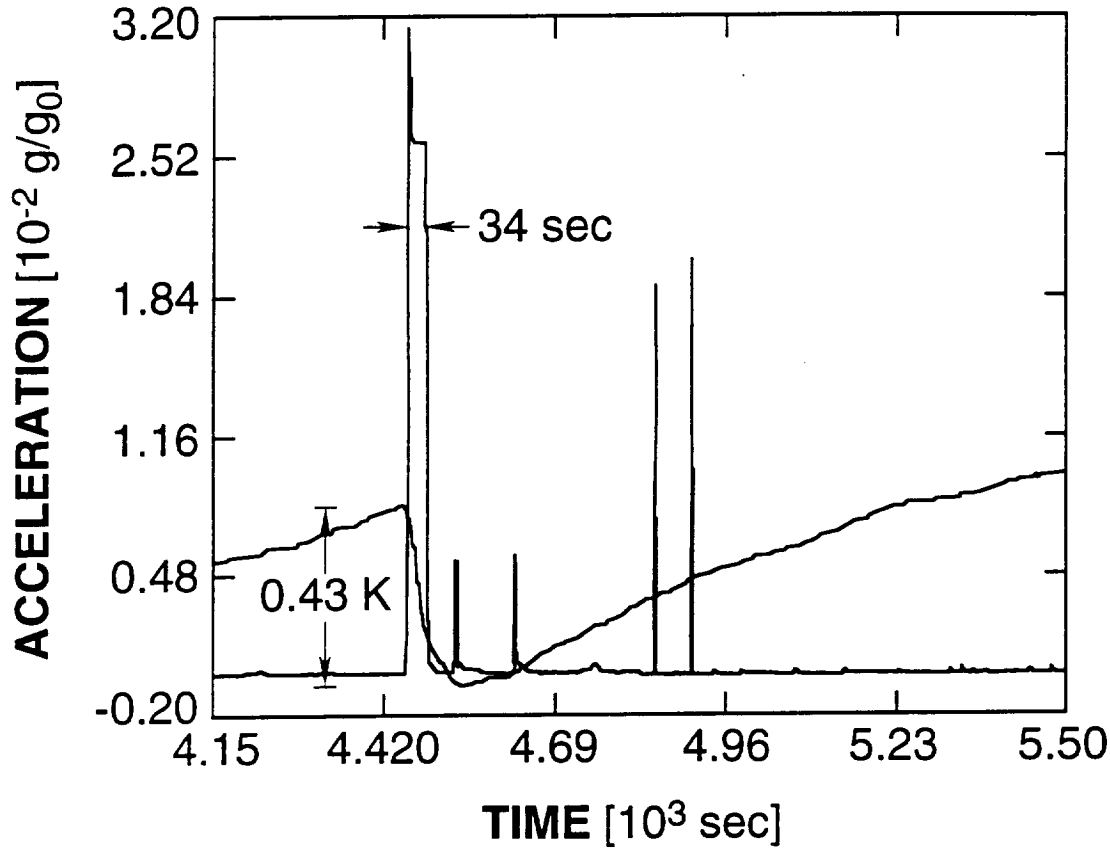

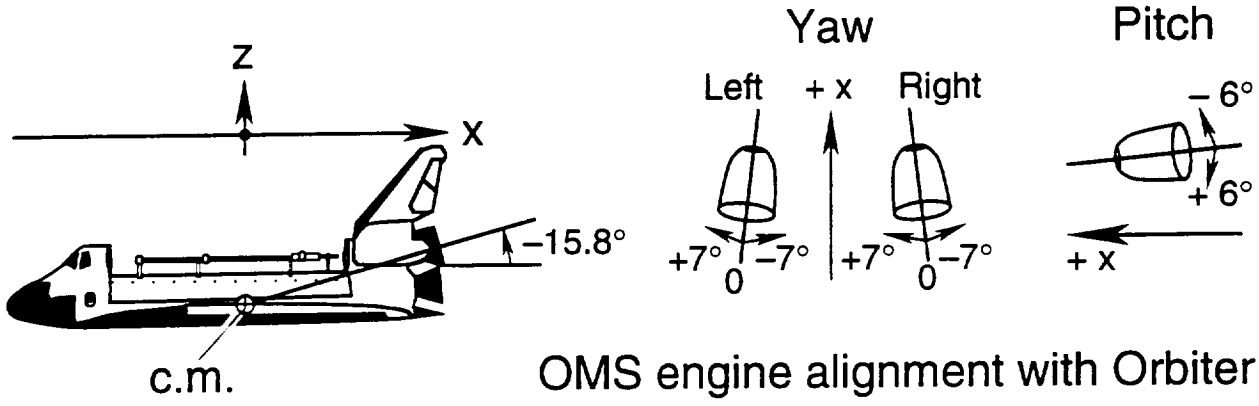

OMS engine alignment with Orbiter

FIG. 2

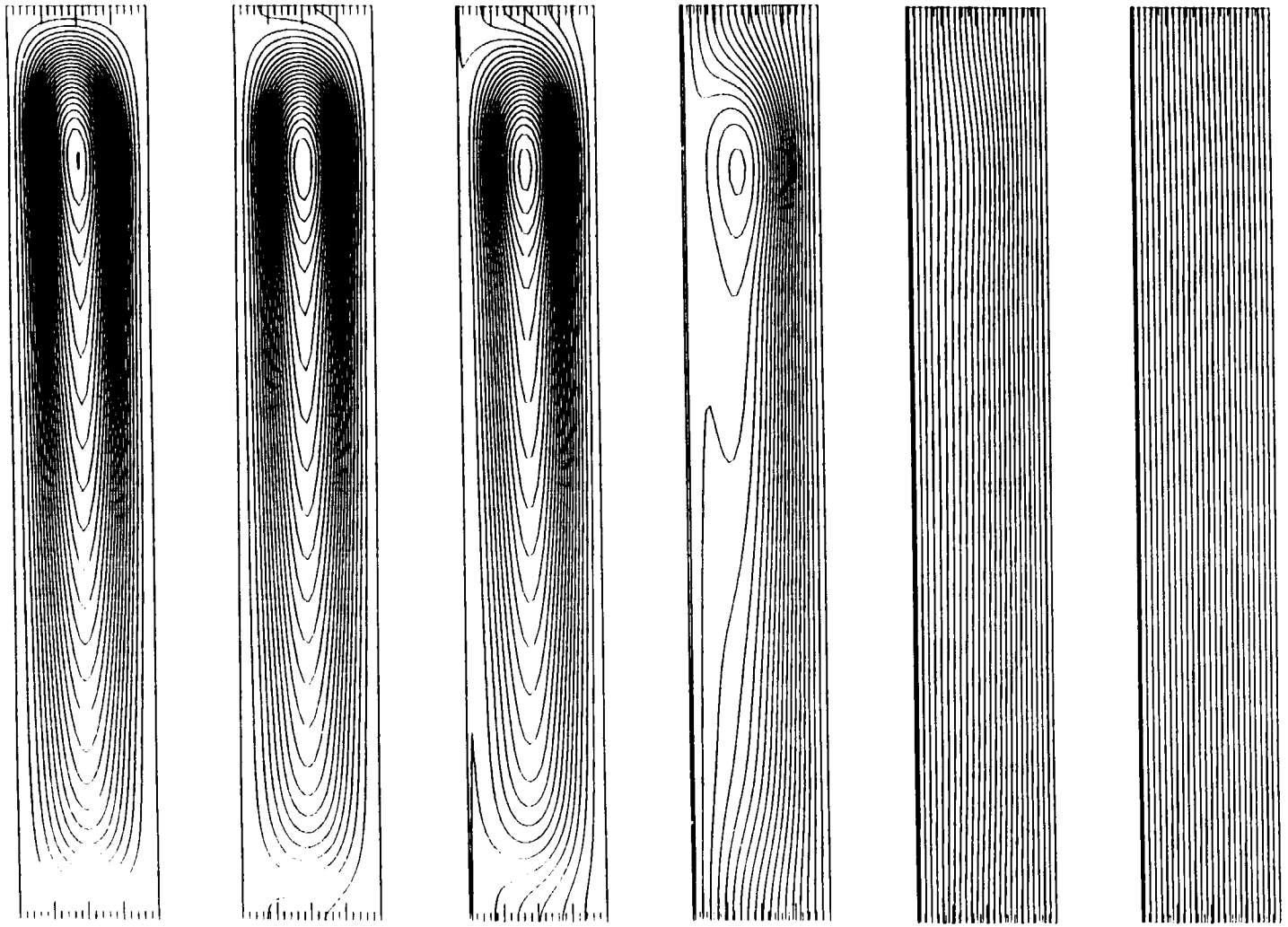

FIG. 3

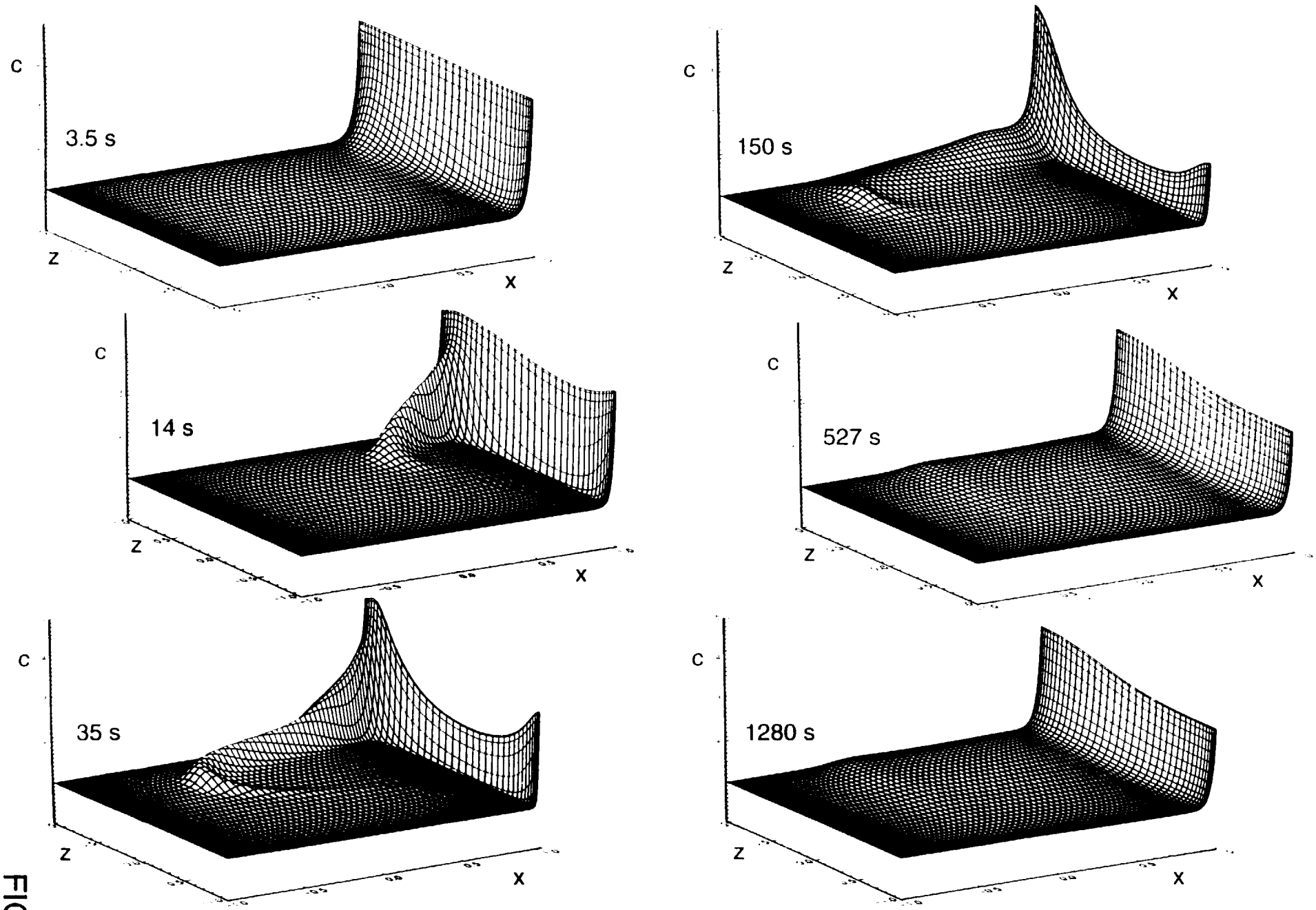

FIG. 4

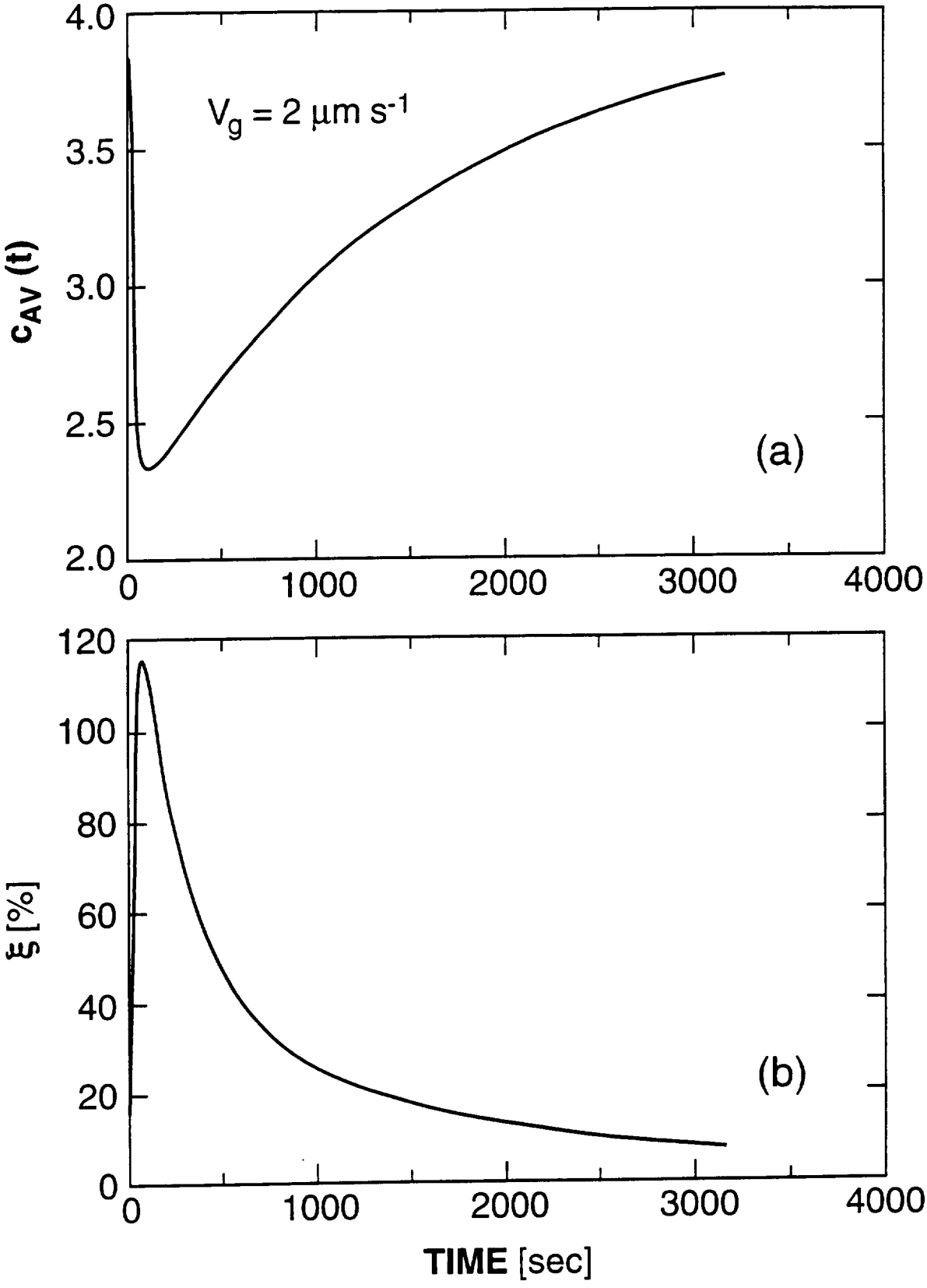
4.0
3.5
3.0
2.5
2.0
$V_g = 2\ \mu m\ s^{-1}$
c_{AV} (t)
(a)
0
1000
2000
3000
4000
120
100
80
60
40
20
0
ξ [%]
(b)
0
1000
2000
3000
4000
TIME [sec]

FIG. 5

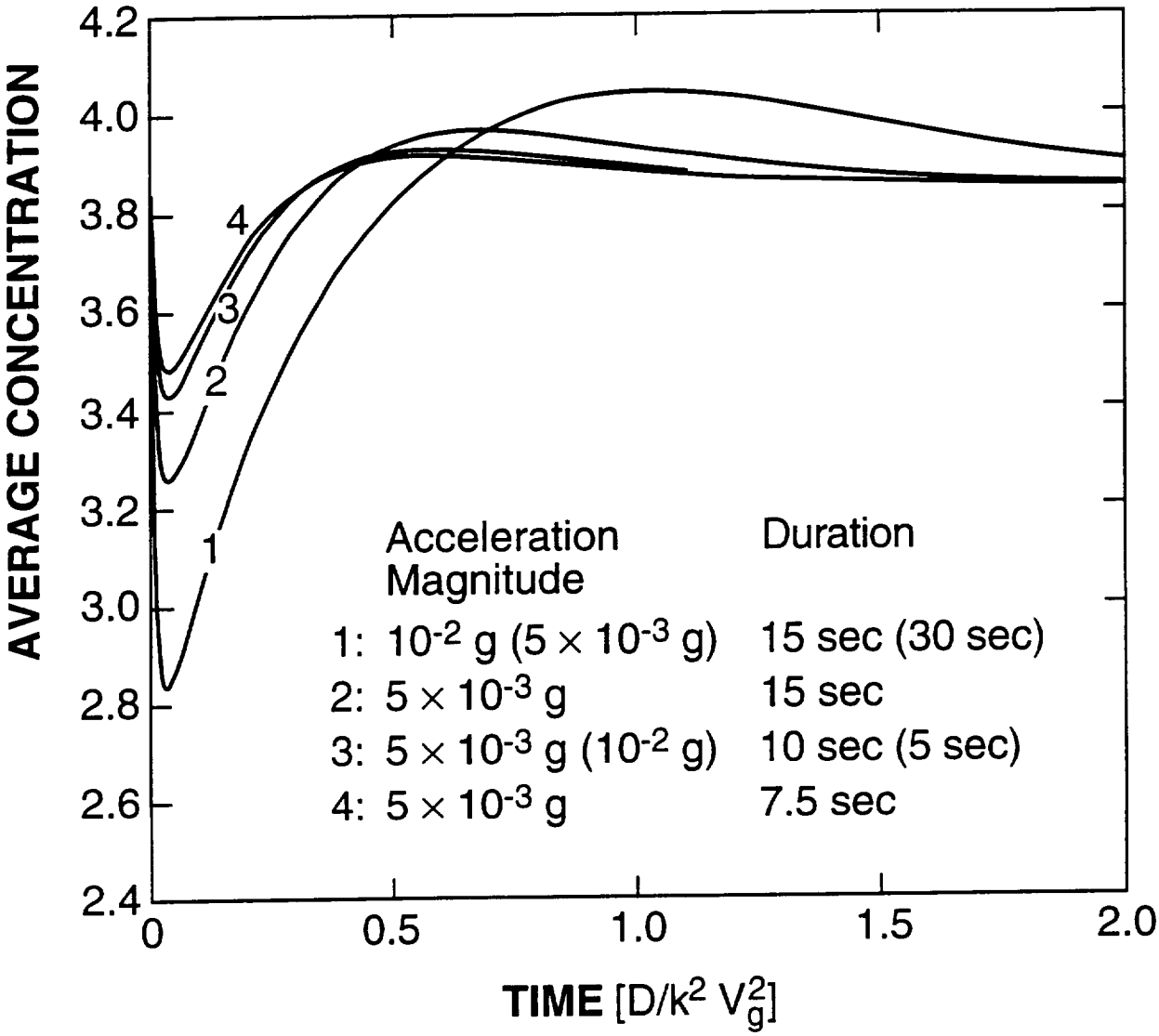
AVERAGE CONCENTRATION
4.2
4.0
3.8
3.6
3.4
3.2
3.0
2.8
2.6
2.4
0
0.5
1.0
1.5
2.0
TIME [D/k² V_g²]
1
2
3
4
Acceleration Magnitude
Duration
1: 10⁻² g (5 × 10⁻³ g)
15 sec (30 sec)
2: 5 × 10⁻³ g
15 sec
3: 5 × 10⁻³ g (10⁻² g)
10 sec (5 sec)
4: 5 × 10⁻³ g
7.5 sec

FIG. 6